Cell. Mol. Biol. (ISSN: 1165-158X)

Journal Homepage: www.cellmolbiol.org

Cellular and Molecular Biology

Original Article

Effects of Leukocyte-rich platelet-rich plasma and Leukocyte-poor platelet-rich plasma on cartilage in a rabbit osteoarthritis model

Kefan Zhang[1], Chenchen Zhang[2], Qiang Ren[1], Dening Wang[1], Li Sun[1] , Xin Wang[3], Yaomin Wang[1], Hui Shi[1*]

[1] Department of Orthopedics and Sports Medicine, Binzhou Medical University Hospital, Binzhou, Shandong, 256603, China
[2] Department of Operating Room, Binzhou Medical University Hospital, Binzhou, Shandong, 256603, China
[3] Department of Orthopedics, Nanyang Central Hospital, Nanyang, Henan, 473000, China

Article Info

Article history:

Received: August 25, 2023
Accepted: December 18, 2023
Published: February 29, 2024

Use your device to scan and read the article online

Abstract

Osteoarthritis is a prevalent chronic disease. One of its primary pathological processes involves the degeneration of articular cartilage. Platelet-rich plasma (PRP) contains cytokines and growth factors that can stimulate the repair and regeneration of articular cartilage tissues. PRP may also slow the progression of osteoarthritis. The purpose of this experiment is to compare the efficacy of Leukocyte poor (LP) - PRP and Leukocyte rich (LR) - PRP in treating rabbit osteoarthritis and to investigate their mechanisms of action. Analyzing the impact of leukocytes on PRP therapeutic effectiveness will provide a valuable clinical reference for the choice of which PRP is better for the treatment of osteoarthritis. A rabbit osteoarthritis model was established by injecting papain into the knee joint cavity, and LP-PRP and LR-PRP were prepared through different centrifugation methods for injection into the knee joint cavity. Eight weeks after injection, rabbit knee cartilage specimens were observed for gross changes, HE staining, senna O-solid green staining, and immunohistochemistry of type II collagen and were quantitatively compared using Pelletier's score, Mankin's pathology score, and ImageJ image processing software. Injection of papain into the knee joint cavity successfully established a rabbit model of osteoarthritis. All three evaluation indexes differed significantly from those of the blank group ($P<0.05$). LP-PRP and LR-PRP exhibited therapeutic effects when compared with the model group. The two PRP groups had similar gross tissue appearance and pathology ($P>0.05$). The LR-PRP group had higher collagen type-II expression ($P < 0.05$) than the LP-PRP group. Both LP-PRP and LR-PRP proved therapeutic for the rabbit papain osteoarthritis model. The difference in leukocyte content between the two groups did not yield different cartilage morphology or other factors by 8 weeks posttreatment. LR-PRP displayed the ability to release more factors relevant to the metabolism of type II collagen than LP-PRP, enabling the preservation of into cartilage collagen content of type II collagen and delaying osteoarthritis progression.

Keywords: Platelet; Osteoarthritis; Rabbits; Cartilage; LP-PRP; LR-PRP

1. Introduction

Osteoarthritis (OA) is a prevalent chronic ailment resulting in pain, swelling, inflammation, and joint dysfunction that affects mobility and daily activities, putting a considerable burden on patients' lives. Millions of people worldwide experience OA, and the number is on the rise (1). With global demographic aging, the prevalence of OA is expected to rise, leading to immense strain on healthcare systems and socioeconomic factors (2). One of the primary causes of OA is the degeneration of articular cartilage, which may result from several factors, such as age, genetic factors, trauma, and joint overuse. Additionally, abnormal joint development, obesity, genetic factors, and lifestyle choices are all risk factors for OA (3).

The pathogenesis and early prevention of OA have recently received significant attention. According to Sanchez-Lopez et al., (4) synovitis can play a crucial role in the cellular and molecular mechanisms underlying the development of early OA. Previous studies have demonstrated a strong correlation between knee instability resulting from meniscus or cruciate ligament injuries in the knee joint and the development of OA. A recent study (5) confirmed this view from the perspective of extensor muscle weakness. Deng et al. (6) suggested that ADAMTS5 gene polymorphism may be associated with the development of knee OA. Studying the pathogenesis and risk factors during the early phase of the disease is crucial for early prevention and treatment.

Besides potential surgical interventions, there are therapies such as pharmaceutical drugs that can entirely halt the progression of this disease. Clinical practice relies heavily on treatments such as exercise therapy, anti-inflammatory medications, hyaluronic acid (HA), and platelet-rich plasma (PRP). Several researchers have focused their attention on alternative pharmaceutical treatments targeted specifically within the knee joint (7). These treatments

* Corresponding author.
E-mail address: sh13475095025@163.com (H. Shi).
Doi: http://dx.doi.org/10.14715/cmb/2024.70.2.31

are believed to offer superior targeting capabilities compared to oral medications, but the therapeutic efficacy of HA remains limited in humans. Numerous scholars have initiated investigations into cytokine therapy associated with cartilage tissue engineering (8). This approach is built upon the study of OA pathogenesis and has led to the development of various specific therapeutic modalities linked to anti-inflammatory factors (9), proinflammatory factors, and signaling pathways (10). One of the latest and increasingly popular therapeutic modalities in clinical practice is mesenchymal stem cell therapy (11). However, Shang et al. (12) demonstrated the limitations and ineffectiveness of stem cell therapy, the potential risks of complications, and the restricted nature of existing research evidence. Consequently, the clinical application of stem cell therapy remains unverified, so it is recommended to approach stem cell therapy with caution until more robust evidence becomes available.

PRP is abundant in growth factors and cytokines, which are biomolecules with the potential to facilitate tissue repair and regeneration. PRP has found widespread utility across various clinical domains (13, 14). Notably, in the treatment of OA, PRP has exhibited superior effectiveness to HA (15). PRP is available in various forms, including leukocyte-poor platelet-rich plasma (LP-PRP), leukocyte-rich platelet-rich plasma (LR-PRP), and platelet-rich fibrin (PRF). These different variants can be prepared using distinct techniques. Backed by an extensive body of research and clinical applications related to PRP, its therapeutic efficacy and safety in addressing OA have gained widespread recognition (16). Expert consensus guidelines on the use of PRP have also been established (17).

However, in clinical practice, the classification and preparation of PRP can be convoluted, with many sources grouping them all together as “PRP.” This practice can inadvertently complicate the evaluation of clinical effectiveness and mechanistic studies of PRP. While some foundational research endeavors have delved into the mechanism of action of PRP (18), more comprehensive investigations are warranted to elucidate their precise modes of action and effects in OA models. In particular, the role of leukocytes in PRP preparations remains a subject of debate, but a better understanding of this could help with the selection of PRP types in clinical settings. Some scholars contend that excessive leukocyte aggregation in joint tissues may lead to pain and inflammation in certain scenarios, while others suggest that leukocytes play a key role in cartilage tissue repair facilitated by PRP. Despite a handful of clinical studies comparing the impact of leukocytes in this context (19), there remains a dearth of animal experiments that could offer deeper insights into the mechanisms at play.

Within this context, the primary objective of this study was to explore the roles of LP-PRP and LR-PRP in a rabbit OA model. Through this comprehensive investigation, we aim to compare the efficacy of LP-PRP and LR-PRP in a rabbit OA model and to shed light on the underlying mechanisms. Our analysis of the influence of leukocytes on the therapeutic effects of PRP will furnish a crucial theoretical foundation for making informed clinical choices regarding the optimal PRP type for the treatment of OA.

2. Materials and Methods

Papain, L-cysteine, hematoxylin and eosin staining solution and modified Senna O-solid green staining kit were supplied by Beijing Solarbio Science & Technology Co., Ltd. Type II collagen primary and secondary antibodies were supplied by Beijing Bioss Biotechnology Company. The optical microscope was supplied by Olympus Company, Japan. The Arthrex ACP system and HORINZON FLEX centrifuge were supplied by Arthrex (Arthrex Inc., Naples, Florida, USA).

2.1. Animals model

The experimental animals were sourced from Jinan Jinfeng Laboratory Animal Co., Ltd. Thirty-two healthy adult New Zealand Rabbits, both male and female, were selected. These rabbits had an age of 4-6 months and a body mass ranging from 2.5-3.1 kg, with an average weight of 2.8±0.3 kg. Throughout the experiment, all New Zealand rabbits were individually housed in cages, ensuring optimal indoor conditions characterized by cleanliness, quietness, ventilation, and dryness. Room temperature was maintained at 20-25°C, and artificial lighting was provided for 12 hours each day. The rabbits were provided unrestricted access to food and water. Prior to group-based model establishment, during a one-week acclimatization period, the animals were given free access to food and water. The OA model was created using the papain method (20) for knee joint cavity injection. A solution consisting of 2:1 (v:v) 4% papain:0.04 mol/L L-cysteine was prepared. On days 1, 4, and 7, 1.0 ml of this solution was injected into the right knee joint cavity of the OA rabbits. Following injection, the rabbits were returned to their cages for standard rearing practices. The model was considered established six weeks after the final injection.

2.2. Preparation of PRP

LR-PRP was prepared following the secondary centrifugation method, as developed by Landesberg et al. (21) In this method, 10 ml of arterial blood was centrifuged at 200 × g for 10 minutes, resulting in the separation of the blood in the tube into three distinct layers: the upper layer comprised the serum, the middle layer contained platelets and leukocytes, and the lower layer consisted of erythrocytes. The erythrocytes located within 2 mm below the middle layer were extracted using a syringe and appropriately disposed of. The remaining specimen was centrifuged at a force of 200 × g for 10 minutes. After centrifugation, 3/4 of the upper section of the serum layer was carefully extracted using a syringe and discarded, leaving the remaining portion as LR-PRP.

LP-PRP was prepared through a single centrifugation procedure. A blood tube containing 10 ml of arterial blood, processed with the Arthrex ACP system, was meticulously positioned within a centrifuge for the initial centrifugation step. This involved subjecting the sample to the following conditions: a centrifugal force of 269×g for 4 minutes. This separated the blood into two distinct layers, the uppermost layer comprising the PRP layer and the lower layer consisting of red blood cells. The upper layer of the sample was taken as the LP-PRP. It underwent precise platelet quantification using a fully automated blood cell analyzer.

2.3. Intraarticular injections

Thirty-two rabbits were randomly allocated into four distinct groups: blank group, model group, LR-PRP group, and LP-PRP group, each group consisting of 8 rabbits, each

with 8 knee joints studied. OA was induced in all groups except for the blank treatment group, employing the papain method. Commencing from the sixth week post-modeling, the model group received 1 mL injections of physiological saline into the joint cavity, the LR-PRP group received injections of LR-PRP, with platelet concentrations ranging from 1, 141-1, 545 × 10^9/L, while the LP-PRP group was administered LP-PRP injections with concentrations within the range of 649-716 × 10^9/L. These injections were administered weekly for three weeks, each dose amounting to 1 mL. The knee joint was moved after administration of the injection solution to ensure that the injection solution was evenly dispersed throughout the joint.

2.4. Observation of cartilage tissue in gross

Following the euthanization of the rabbits 8 weeks post-surgery, a surgical procedure was executed to incise the knee joint capsule. The cartilage of the knee was subjected to visual examination, and cartilage damage was assessed utilizing the Pelletier scoring system (22).

2.5. Cartilage tissue hematoxylin-eosin staining

The bone and articular cartilage samples were excised from the femoral condyle surface. They were fixed using a 40 g/L paraformaldehyde solution, followed by decalcification in EDTA solution. These specimens were then embedded in immersion wax and sliced continuously to achieve a thickness of 5 μm, carefully adjusted by the slicer. To prepare the sections for further analysis, a deparaffinization process was initiated, involving a 10-minute treatment with xylene. The sections were then submerged in water, followed by a wash with xylene. Dehydration was carried out using a gradient of ethanol, involving sequential immersions in 100%, 90%, 80%, and 70% gradient ethanol, with each step lasting for 5 minutes. Next, the sections were rinsed with tap water for 5 minutes. Hematoxylin staining was performed for 5 minutes, after which the sections were rinsed with tap water for 1 minute. Differentiation was achieved through a 1-minute treatment with 5% acetic acid, followed by a 1-minute rinse with tap water. Rebluing was performed using alkaline water for 20 seconds, followed by a 1-minute rinse with tap water. Eosin staining was carried out for 10-20 seconds, followed by another 1-minute rinse with tap water and another round of eosin staining. This final staining procedure took place in alkaline water for 20 seconds, followed by a 1-minute rinse in tap water. Dehydration was accomplished by immersing the sections in ethanol, and they were then made transparent in xylene. The process was concluded by sealing the sections with a drop of neutral gum.

2.6. Cartilage tissue senna-O and solid green stain

The paraffin-embedded sections were deparaffinized as above and subjected to the following staining protocol: The sections were stained with freshly prepared Weigert's staining solution for 3-5 minutes and then washed thoroughly with water. The sections underwent differentiation in an acidic differentiation solution for 15 seconds, followed by a rinse in evaporated water for 10 minutes. They were then immersed in a solid green staining solution for 5 minutes and rapidly washed in a weak acid solution for 10-15 seconds to eliminate any residual solid green. The sections were allowed to air-dry. A saffron staining solution was applied to the sections for 5 minutes. Dehydration was achieved by sequential immersion in 95% ethanol for 2-3 seconds, anhydrous ethanol for 2-3 seconds, and finally anhydrous ethanol for 1 minute. The stained sections were rendered transparent in xylene and sealed using an optical resin. Alterations in cartilage structure, cell arrangement, matrix staining, and tidemark integrity were assessed utilizing Mankin's pathology scoring system (23).

2.7. Immunohistochemistry for type II collagen in cartilage tissue

Paraffin sections were subjected to heating in an oven at 60°C for 30-60 minutes, then sequentially immersed in three changes of xylene (xylene I, xylene II, and xylene III) for 10 minutes each. This was followed by an ethanol gradient wash, with 100% ethanol followed by 95%, 80%, and 70%, each concentration being applied for 2 minutes. The sections were then rinsed in distilled water for 5 minutes. To reduce endogenous peroxidase activity, the sections were washed three times with PBS for 3 minutes each. The next step involved the incubation of the sections in a prewarmed closed permeabilization solution (comprising 40 ml PBS and 400 μl of 30% H_2O_2) for 30 minutes. Following this step, the sections were washed with PBS three times for 3 minutes. To unmask the antigenic sites, the sections were immersed in 0.01 M sodium citrate buffer at pH 6.0, boiled, and then allowed to cool naturally to room temperature. Subsequently, they were washed with PBS three times for 3 minutes each time. To block any nonspecific binding sites, serum from the same source as the secondary antibody was applied to the tissue. The tissue was treated with diluted serum and incubated at 37°C for 30 minutes, after which excess serum was removed using filter paper. The tissue was then incubated with 20 μl of diluted primary antibody overnight at 4°C. After primary antibody incubation, the sections were washed with PBS three times for 3 minutes. Next, the sections were incubated with the secondary antibody. Specifically, 20 μl of diluted secondary antibody was added dropwise to the tissue sections, and the incubation was carried out at 37°C for 2 hours. The sections were washed with PBS three times for 3 minutes each time. For color development, the sections were treated with DAB-H_2O_2 for 5 minutes. During this step, it was essential to observe the staining under a microscope to ensure its adequacy. Color development could be stopped by rinsing with distilled water within 10 minutes. The sections were then stained with Mayer hematoxylin for 30 seconds, followed by a water wash. They were differentiated in hydrochloric acid–alcohol for 2 seconds and then rinsed in running water for 15 minutes. To dehydrate the sections, an ethanol gradient was used, starting from lower concentrations and increasing to 50%, 70%, 95%, and 100%, each concentration being applied for 2 minutes. Xylene was employed for a 5-minute period to render the sections transparent. Finally, neutral gum was applied to seal the sections.

ImageJ image analysis software was employed for the analysis of microscopic brownish-yellow particles, indicative of positive type II collagen expression. Semiquantitative analysis was performed by selecting a blank region in each section for reference, and the average integral optical density of the positive reaction was determined by selecting five nonoverlapping fields of view under high magnification (400×). The mean integral optical density of the positive area rate from these five fields of view was taken

as the measurement of type II collagen expression for that specific section.

2.8. Statistical analysis

SPSS version 21.0 software was utilized for statistical analysis and creation of the database. The measurement data are presented as mean ± standard error. Analysis of variance (ANOVA) was conducted to compare multiple groups, and was employed for further analysis between two groups. Significance was attributed to P values < 0.05.

3. Results

3.1. Macroscopic observation of cartilage tissue

The macroscopic observation of cartilage tissue is shown in Figure 1. The blank group exhibited minimal yellowish joint fluid within the joint cavity, along with a smooth articular cartilage surface devoid of noticeable fissures. There was no evident formation of bony protrusions at the joint's edge, and synovial membrane hyperplasia was not apparent. In the model group, the joint cavity fluid appeared yellow, the articular cartilage surface took on a grayish hue, and it exhibited a rough texture with discernible fissures. A modest degree of bone crenellation had formed at the joint's periphery, some damage extending to the cartilage's deep layer and partial exposure of subcartilaginous bone. Synovial hyperplasia and thickening were evident. The articular cartilage surface in the LP-PRP group displayed a pale white appearance, with transparent and smooth cartilage surfaces characterized by small surface fissures. Synovial thickening was slight. Conversely, the LR-PRP group featured minimal effusion, articular cartilage surfaces that were not uniformly smooth, and some with discernible fissures. Various degrees of synovial hyperplasia were observed.

The relevant scoring statistics are shown in Table 1. A comparison of Pelletier scores derived from visual cartilage tissue observations revealed statistical differences between multiple groups, except for the absence of a significant difference between the LP-PRP and LR-PRP groups (P < 0.05). These findings suggest that both LP-PRP and LR-PRP exhibited therapeutic effects compared to the model group, with no marked disparity in their therapeutic efficacy (P > 0.05).

In the analysis of Pelletier score, Mankin's score, and Type II Collagen IOD data, significant statistical differences were observed among the experimental groups. Both LP-PRP and LR-PRP groups exhibited variations in Pelletier score and Mankin's score compared to the blank Group and model Group, indicating therapeutic and protective effects on cartilage. However, the distinction between the two PRP groups was not deemed statistically significant. Notably, there were discernible disparities in the levels of Type II Collagen IOD between the two groups, with the LR-PRP Group demonstrating superior efficacy in preserving Type II Collagen. This difference reached statistical significance when compared to the LP-PRP Group.

3.2. Pathological observation of hematoxylin-eosin staining and senna O-solid green staining of cartilage tissue

The pathological observation of hematoxylin-eosin staining and senna O-solid green staining of cartilage tissue is shown in Figures 2 and 3. In the blank group, the articular cartilage surface displayed a smooth and even appearance. The four layers of the surface, transitional zone, radiolucent zone, and calcified zone exhibited well-defined structures with regular arrangement. The cell distribution and staining were uniform, and the tidemark was intact. No blood vessels traversed the articular cartilage. The cartilage had regular morphology, with orderly chondrocyte morphology and distribution. In the model group, the articular cartilage surface was severely damaged, the cartilage layer showing extensive detachment and disruption of the structural layers. Fissures extended deep into

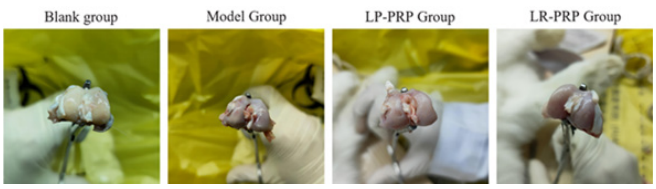

Fig. 1. Macroscopic observation of cartilage tissue. In the macroscopic observation of cartilage tissue, the blank group exhibited no significant changes, presenting a smooth and normal appearance. In contrast, the model group displayed the most severe signs of osteoarthritis, characterized by an uneven surface and darkened color. The LP-PRP Group and LR-PRP Group exhibited intermediary conditions, falling between the extremes observed in the blank and model groups.

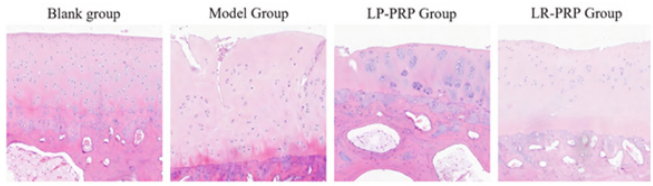

Fig. 2. Pathological observation of hematoxylin-eosin staining of cartilage tissue. In the pathological observation of hematoxylin-eosin staining of cartilage tissue, We conducted a 100x observation using an optical microscope, the blank group exhibited no notable changes, displaying a smooth cartilage surface. The model group presented the most pronounced manifestation of osteoarthritis, characterized by an uneven surface and darkened color. The LP-PRP Group and LR-PRP Group displayed intermediate conditions, with a noticeable occurrence of chondrocyte aggregation in both groups.

Table 1. Summary of scores for each group.

Score	Group				F	P
	Blank Group	Model Group	LP-PRP Group	LR-PRP Group		
Pelletier score	0.1250±0.3536	3.0000±0.5345[a]	2.3750±0.5176[a, b]	2.2500±0.7071[a, b]	42.566	<0.001
Mankin's score	0.3750±0.5176	10.7500±1.2817[a]	6.7500±0.8864[a, b]	6.8750±1.4577[a, b]	122.543	<0.001
Type II Collagen IOD	0.1847±0.0134	0.1063±0.0087[a]	0.1318±0.0057[a, b]	0.1413±0.0060[a, b, c]	103.7	<0.001

a: P < 0.05 compared to the blank group; b: P < 0.05 compared to the model group; c: P < 0.05 compared to the LP-PRP group.

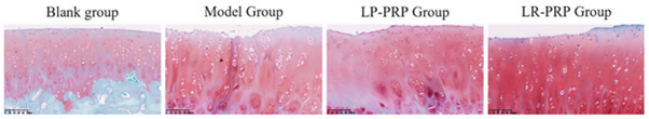

Fig. 3. Pathological observation of senna O-solid green staining of cartilage tissue. In the pathological observation of senna O-solid green staining of cartilage tissue, observations were conducted at 200x magnification using an optical microscope. The blank group exhibited typical cartilage tissue with a smooth surface. Conversely, the model group displayed a concave cartilage surface with evident cracks and disorganized arrangement of cartilage cells. Both the LP-PRP Group and LR-PRP Group exhibited notable chondrocyte aggregation. Notably, all groups, except the blank group, presented uneven staining patterns.

the radiolucent zone of the femoral condyles, accompanied by the presence of numerous chondrocyte clones. The cell distribution and arrangement were irregular, and the total cell count was reduced. The tidemark was distorted and advanced, with the infiltration of blood vessels. Staining was moderately uneven, chondrocytes were relatively few, and they were disorganized. The articular surface exhibited irregular morphology, with some areas displaying fissures. Changes in cartilage morphology were observed in the LP-PRP group. Some chondrocytes on the cartilage surface exhibited a more orderly arrangement, increased cell numbers, and some chondrocyte clustering with the formation of chondrocyte-like cells. Staining was relatively uniform. Cartilage morphology was altered in the LR-PRP group, some areas of its articular cartilage surface show depressions and elevations. Chondrocyte morphology was more regular, but cell arrangement was somewhat disordered. Some chondrocytes clustered, and the tidemark exhibited more distortion. The staining was lighter.

The statistical information of Mankin's pathological scores is shown in Table 1. In the comparison of Mankin's pathological scores, as with the macroscopic observations, there were statistically significant differences between the multiple groups ($P < 0.001$). The pathological scores were still similar between the LP-PRP and LR-PRP groups ($P > 0.05$), while the comparisons between all other group pairs exhibited significant differences ($P < 0.05$). This indicates that the rabbit OA model was successfully established using the papain method, as it had significant differences from the blank control group ($P > 0.05$).

3.3. Immunohistochemical expression of type II collagen in cartilage tissue

The immunohistochemical expression of type II collagen in cartilage tissue is shown in Figure 4 and the statistics of IOD values are shown in Table 1. In the assessment of the integral optical density (IOD) of type II collagen, a statistically significant difference was observed between multiple groups. Furthermore, pairwise comparisons between groups demonstrated statistically significant distinctions ($P < 0.05$). Type II collagen expression within articular cartilage exhibited the highest levels in the blank group, the lowest in the model group, and intermediate levels in the LR-PRP and LP-PRP groups. The mean type II collagen IOD in the articular cartilage of the blank group was significantly different from that of the model group ($P < 0.05$), indicating degenerative changes in the joints modeled in the animal experiments. Comparatively, the type II collagen IOD in the articular cartilage of the LR-PRP or LP-PRP group was significantly different from the value of the model group ($P < 0.05$), implying that the treatment in these two groups exhibited a protective or therapeutic effect against the rabbit OA model induced by papain. The blank group showed a notably higher expression of type II collagen ($P < 0.05$).

4. Discussion

As the incidence of OA continues to rise, the socioeconomic burden associated with it is gradually increasing (1). Consequently, there has been a surge in recent years in studies focusing on the pathogenesis of OA, as well as the exploration of new treatment modalities and therapeutic targets. The etiology of OA is multifaceted. Wang and He (24) found that obesity places additional mechanical stress on tibial and femoral cartilage, increasing the risk of OA, and is associated with elevated inflammatory factors. Loeser et al. (25) demonstrated that multiple processes in the progression of OA promote a pro-inflammatory, catabolic state, rendering the joint tissues more susceptible to cell death, thereby accelerating tissue destruction and hindering the repair of damaged matrix, ultimately contributing to OA development. Traumatic factors, such as meniscus and anterior cruciate ligament injuries, which result in knee instability, will further exacerbate OA development and have been linked to complement activation and mast cell and macrophage hyperplasia (26). In a previous rabbit OA model (27), anterior cruciate ligament transection and meniscectomy were employed to induce OA by destabilizing the rabbit knee joint and causing subchondral bone loss (28). In contrast, we utilized the papain method to induce rabbit OA. This method dates back several decades, including Havdrup and Telhag study (29), which demonstrated that concentrated papain injections into the joint cavity could rapidly induce changes in articular cartilage. Lesions caused by papain at low concentrations bear similarities to human OA, making it a favorable choice for studying early degeneration and repair changes in OA. Furthermore, it is more conducive than other methods to the examination of articular cartilage metabolism in the early stages of joint diseases. Hermeto et al. (30) investigated both modeling approaches and confirmed that both methods successfully model OA. They found that the intra-articular injection method provided greater sta-

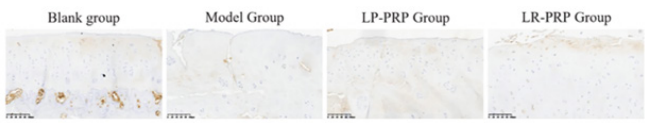

Fig. 4. Immunohistochemical expression of type II collagen in cartilage tissue. In immunohistochemical expression of type II collagen in cartilage tissue, observations were conducted at 200x magnification using an optical microscope. The blank group exhibited the highest and most evenly distributed presence of type II collagen within the cartilage. In contrast, the model group displayed the least amount of type II collagen, distributed unevenly. Both the LP-PRP Group and LR-PRP Group fell in between these extremes. Notably, the type II collagen in the LP-PRP Group cartilage demonstrated a uniform decrease compared to the blank group. On the other hand, the LR-PRP Group exhibited more occurrences of type II collagen on the cartilage surface compared to the LP-PRP Group.

bility and control than surgical interventions. In line with our experimental results, eight weeks after papain injection into the knee joint cavity, the model group exhibited observable changes in cartilage morphology and a notable reduction in chondrocytes upon cartilage tissue staining, distinguishing it from the blank treatment group. This underscores the method's ability to establish a stable rabbit knee OA model with remarkable stability.

In clinical practice, the absence of disease-modifying osteoarthritis drugs (DMOADs) for OA has led to the adoption of treatments such as intra-articular injections of HA and PRP for early OA management. PRP, originally introduced in dentistry, has since found widespread application in various medical fields, notably orthopedics and sports medicine (31). PRP contains an abundance of growth factors, chemokines, and proinflammatory cytokines, as demonstrated by Riewruja et al. (32) and others, which seem to promote the resolution of inflammation, bolstered by anti-inflammatory cytokines and regenerative growth factors that subsequently slow the progression of OA. Various in vivo findings suggest that PRP could influence the anabolic environment within joints, providing the necessary bioactive molecules to maintain joint homeostasis, alleviate pain, and enhance joint function. Moussa et al. (33) proposed that PRP, by activating α-granules and promoting the release of specific proteins, can stimulate the synthesis of the cartilage matrix. This stimulation occurs through binding to corresponding receptors on collagen, osteoblasts, and chondrocytes, ultimately driving cartilage matrix synthesis and tissue regeneration, which leads to chondroprotection. It is postulated that the effectiveness of PRP is enhanced in the presence of stem cells. In modern practice, PRP remains a valuable complement to mesenchymal stem cell (MSC) therapy. Ragni et al. (34) cultured bone marrow stromal stem cells with PRP and found that they released therapeutic molecules, forming the foundation for this innovative combination of agents for OA treatment. Beigi et al. (35) conducted in vitro experiments that demonstrated the efficacy of stem cells combined with PRP in promoting enhanced cartilage repair in a rabbit cartilage injury model.

Among the various biologic therapies, intra-articular PRP injection has gained increasing attention as an alternative treatment for knee OA, surpassing surgical interventions and demonstrating superior clinical outcomes compared to sodium hyaluronate. Liu et al. (36) revealed that PRP exhibited superior effects in repairing damaged cartilage and subchondral bone when compared to sodium hyaluronate. The recent meta-analysis conducted by Peng et al. (37) demonstrated that PRP yielded better overall outcomes for knee OA than HA at 3, 6, and 12 months of follow-up. Wang et al. (38) followed up patients for 7 years and found that PRP was better than HA in survival and reintervention rates, VAS score, and WOMAC score. Notably, while there were no significant disparities in imaging assessments between the two treatment approaches, patients treated with PRP expressed higher satisfaction levels than those receiving HA.

PRP can be classified into different types, including LP-PRP, LR-PRP and PRF, depending on the specific preparation method (39). For conditions such as OA, both LP-PRP and LR-PRP are frequently employed in clinical practice. However, there is a notable absence of fundamental experimental investigations comparing the effects of these two PRP types on OA, which this study aimed to rectify. PRP can be prepared by various techniques. LR-PRP is often obtained through a two-step centrifugation process. Tamimi et al. (40) noted that double centrifugation yielded higher platelet concentrations than single centrifugation, although the former yielded greater variability. Furthermore, an analysis of the ultrastructure of PRP via transmission electron microscopy revealed that the double centrifugation method induced changes in the ultrastructure of PRP during the centrifugation process, rendering it more susceptible to minor errors during preparation. Similar conclusions were drawn from the experimental findings of Nagata et al. (41) regarding the centrifugation of blood from New Zealand Rabbits. Nevertheless, PRP preparation protocols remain a topic of debate, and a standardized protocol has yet to be established. Piao et al. (42) proposed a theoretical framework for predicting platelet and leukocyte recoveries during the centrifugation of whole blood from test tubes for PRP preparation. Ozer et al. (43) aimed to optimize PRP preparation by adjusting the centrifugal force and duration. They argued that platelets should be evaluated based on platelet mass, rather than platelet concentration alone, and in conjunction with mean platelet volume. All centrifugation forces and durations can yield bioreactive PRP, and it is suggested that if high centrifugation forces are employed, shorter durations should be chosen, while lower forces should be paired with longer centrifugation times. In this study, LR-PRP was prepared using the Landesberg et al. (21) method, and LP-PRP was prepared using the Arthrex ACP system (44). Both types of PRP met the specified criteria. LR-PRP achieved a platelet concentration up to 5 times that of whole blood, accompanied by a greater leukocyte concentration than whole blood had. LP-PRP reached a platelet concentration 2.5 times that of whole blood but contained few leukocytes. A variety of commercial centrifugal devices are available for preparing PRP that meet specific requirements. In a study by Harrison et al., (45) an examination of PRP compositions prepared using different commercial devices revealed that six distinct single-spin PRP preparation methods could attain the desired yield, the choice of method being contingent on the specific clinical application and disease considerations.

Clinical studies on the role of leukocytes in PRP have yielded mixed results. Riboh et al. (19) conducted a meta-analysis comparing the clinical outcomes and adverse effect incidence of LP-PRP and LR-PRP in knee OA. They concluded that both LP-PRP and LR-PRP outperformed HA treatment in delivering improved clinical outcomes. Notably, the LP-PRP group more significantly improved their WOMAC score, and the data suggested that the safety of PRP might not be directly linked to leukocyte concentration. This conclusion was corroborated in our study, where we observed no adverse effects, such as fatalities, in New Zealand Rabbits following the injection of LP-PRP or LR-PRP, both treatments being well tolerated. Jayaram et al. (46) found that in a murine model of surgically induced OA, repeated postoperative intra-articular administration of LP-PRP led to moderate reductions in OARSI and synovitis scores. However, phase-contrast micro-CT analysis revealed that LP-PRP treatment offered protection against cartilage volume and surface loss, with values akin to those of sham mice. Despite greater protection against cartilage pathology and loss, LP-PRP was

more effective in preventing the development of thermal nociceptive hypersensitivity at various postoperative time points. In our experiment, the injection of either LR-PRP or LP-PRP 6 weeks after papain injection showed positive therapeutic effects compared to untreated rabbit knee cartilage, as observed visually and in histological examinations. The morphology and volume scores of cartilage surfaces in some rabbit knee cartilages in the LP-PRP group approached those of the blank group. However, when considering cell counts and tidemark line staining scores collectively, there was no substantial difference in treatment effects between LR-PRP and LP-PRP.

In a double-blind comparative trial conducted by Di Martino et al. (47), LP-PRP was prepared using a leukocyte filter and achieved platelet concentrations equivalent to those of LR-PRP. Their study showed that three intra-articular injections of either LR-PRP or LP-PRP yielded nearly identical clinical outcomes in patients with knee OA over a 12-month follow-up period. Adverse event rates were similarly low in both treatment groups. The presence of leukocytes did not significantly impact the clinical outcomes of PRP injections. Nevertheless, animal model experiments may unveil more nuanced cartilage differences. In our study, both PRP treatment groups displayed more organized chondrocyte arrangements compared to the model group, along with the presence of multiple chondrocyte aggregates. We inferred that differences in leukocyte content between the two types of PRP were not the primary cause of variations in cartilage repair. Furthermore, Lana et al. (48) argued against the use of LP-PRP in knee OA treatment, suggesting that specific leukocytes play a crucial role in the inflammatory process preceding tissue regeneration by releasing relevant pro- and anti-inflammatory molecules. They also proposed that the combination of neutrophils and activated platelets might have a more positive impact on tissue repair and highlighted the importance of monocyte plasticity in noninflammatory and reparative roles in tissue repair. While we did not directly compare the inflammatory response after knee OA induction, we recognize that PRP has the capacity to release numerous anti-inflammatory and pro-inflammatory factors. Therefore, evaluating the inflammatory response in the rabbit joint cavity, including the arthritic fluid and synovium, as well as assessing the release of inflammatory factors, will be the direction of future research.

Articular cartilage, a thin connective tissue layer measuring 1-3 mm thick, covers the ends of long bones and withstands repetitive mechanical loads characterized by high shear, tensile, and compressive strains. The maintenance of low friction between cartilages depends on both the cartilage's structural composition and the lubrication provided by joint fluid. The structure of articular cartilage comprises a supramolecular network of collagen fibers, primarily type II collagen, enveloped within a gel of proteoglycans and water. Type II collagen constitutes approximately 80% of the total collagen content and plays a critical role in providing mechanical stability to cartilage (49). Its absence in articular cartilage can lead to excessive collagen degradation by matrix metalloproteinases (MMPs), causing damage to cartilage tissue. A prospective study by Sadigursky et al. (50) demonstrated that undenatured type II collagen (UC-II) improved pain, joint stiffness, and overall quality of life in 60- to 80-year-old patients with knee OA after a 90-day treatment, as also corroborated by Xu et al. (51) The current body of research on type II collagen underscores its significant role in OA progression. Our experimental study likewise focused on type II collagen expression. In the immunohistochemical staining for type II collagen, both the LR-PRP and LP-PRP groups preserved more type II collagen than the model group. Notably, LR-PRP exhibited a more pronounced positive effect. In a study by Orhan et al. (52) on a rat OA model, inflammation and pain in osteoarthritic joints were alleviated through the reduction of inflammatory mediators following oral administration of undenatured type II collagen. The study also established that type II collagen functions by inhibiting inflammatory factors and mediators linked to the NF-κB signaling pathway, such as COX-2 and PGE2. Nagata et al. (53) found, by studying pure knockout mice of Runx2, that a decrease in type II collagen expression accelerated OA. We hypothesize that the growth factors in PRP may inhibit factors and mediators associated with the NF-κB signaling pathway. This inhibition reduces pathway activation, inhibits Runx2 gene expression, lessens type II collagen degradation, and consequently hinders the progression of OA.

Here, LR-PRP prepared using the Landesberg method exhibited a higher platelet concentration than LP-PRP prepared through a single-centrifugation approach. However, the potential impact of prolonged centrifugation time on platelet activity remains uncertain. It is now widely acknowledged that the therapeutic effectiveness of PRP in OA primarily arises from the release of numerous growth factors and cytokines by platelets. However, the specific types and quantities of growth factors liberated in PRP obtained through these two different methods are not yet fully characterized.

Comprehensive investigations concerning the role of cytokines in OA are ongoing (8, 54). Furthermore, it has become apparent that the therapeutic efficacy of PRP for a given disease may depend on the specific genetic phenotype of the patient (55). Researchers such as Riewruja et al. (32) are actively exploring the varieties of growth factors enriched in PRP. Future research on PRP should be directed toward a thorough exploration of the individual roles of various cytokines and growth factors in PRP. Understanding how these distinct components influence the pathogenesis and pain associated with OA is of paramount importance. This knowledge can be harnessed to optimize these components for enhanced therapeutic effects.

5. Conclusion

Both LP-PRP and LR-PRP exerted therapeutic benefits in a rabbit OA model established through the papain method. Within 8 weeks of treatment, the disparity in leukocyte content between the two formulations did not yield discernible differences in cartilage morphology or other parameters. Notably, LR-PRP demonstrated a superior capacity to release factors associated with type II collagen metabolism, preserving the type II collagen content within the cartilage and effectively retarding the progression of OA, when compared to LP-PRP.

Acknowledgments

This work has been funded by the Shandong Provincial Key Clinical Specialized Discipline Construction Project, the Shandong Province Medical and Health Technology Development Plan Project, 2020 Industrial University

Collaborative Education Project, and Binzhou Medical University Xu Rongxiang Regenerative Medicine Development Plan Project. We appreciate the guidance provided by experts from the Department of Osteoarthritis and Sports Medicine at the Affiliated Hospital of Binzhou Medical College for the experiment, as well as the assistance provided by the Medical Experimental Center of the Affiliated Hospital of Binzhou Medical College for the experiment.

Data availability statement

The authors confirm that the data supporting the findings of this study are available within the article or its supplementary materials.

Funding statement

Shandong Provincial Key Clinical Specialized Discipline Construction Project (SLCZDZK-0302)
Shandong Province Medical and Health Technology Development Plan Project (2017WS040)
2020 Industry-University Collaborative Education Project (202002204024)
Binzhou Medical University Xu Rongxiang Regenerative Medicine Development Plan Project (BY2019XRX04)

Conflict of interest disclosure

All authors declare that there are no conflicts of interest during the research and article writing process. The funding support for the project did not affect the viewpoint of the article and the statistical analysis and reporting of the objective results of the research data.

Ethics approval statement

The experiment was approved by the Ethics Committee of Binzhou Medical University Affiliated Hospital with approval number 20220929.

References

1. Hunter DJ, March L, Chew M. Osteoarthritis in 2020 and beyond: a Lancet Commission. Lancet. 2020;396(10264):1711-1712. doi: 10.1016/S0140-6736(20)32230-3.
2. Giorgino R, Albano D, Fusco S, Peretti GM, Mangiavini L, Messina C. Knee Osteoarthritis: Epidemiology, Pathogenesis, and Mesenchymal Stem Cells: What Else Is New? An Update. Int J Mol Sci. 2023;24(7). doi: 10.3390/ijms24076405.
3. Werner DM, Golightly YM, Tao M, Post A, Wellsandt E. Environmental Risk Factors for Osteoarthritis: The Impact on Individuals with Knee Joint Injury. Rheum Dis Clin North Am. 2022;48(4):907-930. doi: 10.1016/j.rdc.2022.06.010.
4. Sanchez-Lopez E, Coras R, Torres A, Lane NE, Guma M. Synovial inflammation in osteoarthritis progression. Nat Rev Rheumatol. 2022;18(5):258-275. doi: 10.1038/s41584-022-00749-9.
5. Oiestad BE, Juhl CB, Culvenor AG, Berg B, Thorlund JB. Knee extensor muscle weakness is a risk factor for the development of knee osteoarthritis: an updated systematic review and meta-analysis including 46 819 men and women. Br J Sports Med. 2022;56(6):349-355. doi: 10.1136/bjsports-2021-104861.
6. Deng T, Zhou Y, Zhang K, Dong Z, Zhang J, Lv X, et al. Association of polymorphisms in ADAMTS-5 gene with the susceptibility to knee osteoarthritis: A protocol for systematic review and meta-analysis. Medicine (Baltimore). 2021;100(49):e28188. doi: 10.1097/MD.0000000000028188.
7. Nowaczyk A, Szwedowski D, Dallo I, Nowaczyk J. Overview of First-Line and Second-Line Pharmacotherapies for Osteoarthritis with Special Focus on Intra-Articular Treatment. Int J Mol Sci. 2022;23(3). doi: 10.3390/ijms23031566.
8. Liu S, Deng Z, Chen K, Jian S, Zhou F, Yang Y, et al. Cartilage tissue engineering: From proinflammatory and anti-inflammatory cytokines to osteoarthritis treatments (Review). Mol Med Rep. 2022;25(3). doi: 10.3892/mmr.2022.12615.
9. Wu H, Peng Z, Xu Y, Sheng Z, Liu Y, Liao Y, et al. Engineered adipose-derived stem cells with IGF-1-modified mRNA ameliorates osteoarthritis development. Stem Cell Res Ther. 2022;13(1):19. doi: 10.1186/s13287-021-02695-x.
10. Malemud CJ. Anticytokine therapy for osteoarthritis: evidence to date. Drugs Aging. 2010;27(2):95-115. doi: 10.2165/11319950-000000000-00000.
11. Wei P, Bao R. Intra-Articular Mesenchymal Stem Cell Injection for Knee Osteoarthritis: Mechanisms and Clinical Evidence. Int J Mol Sci. 2022;24(1). doi: 10.3390/ijms24010059.
12. Shang Z, Wanyan P, Zhang B, Wang M, Wang X. A systematic review, umbrella review, and quality assessment on clinical translation of stem cell therapy for knee osteoarthritis: Are we there yet? Stem Cell Res Ther. 2023;14(1):91. doi: 10.1186/s13287-023-03332-5.
13. Peerbooms JC, Lodder P, den Oudsten BL, Doorgeest K, Schuller HM, Gosens T. Positive Effect of Platelet-Rich Plasma on Pain in Plantar Fasciitis: A Double-Blind Multicenter Randomized Controlled Trial. Am J Sports Med. 2019;47(13):3238-3246. doi: 10.1177/0363546519877181.
14. Chen X, Jones IA, Park C, Vangsness CT, Jr. The Efficacy of Platelet-Rich Plasma on Tendon and Ligament Healing: A Systematic Review and Meta-analysis With Bias Assessment. Am J Sports Med. 2018;46(8):2020-2032. doi: 10.1177/0363546517743746.
15. Belk JW, Kraeutler MJ, Houck DA, Goodrich JA, Dragoo JL, McCarty EC. Platelet-Rich Plasma Versus Hyaluronic Acid for Knee Osteoarthritis: A Systematic Review and Meta-analysis of Randomized Controlled Trials. Am J Sports Med. 2021;49(1):249-260. doi: 10.1177/0363546520909397.
16. Smith PA. Intra-articular Autologous Conditioned Plasma Injections Provide Safe and Efficacious Treatment for Knee Osteoarthritis: An FDA-Sanctioned, Randomized, Double-blind, Placebo-controlled Clinical Trial. Am J Sports Med. 2016;44(4):884-891. doi: 10.1177/0363546515624678.
17. Eymard F, Ornetti P, Maillet J, Noel E, Adam P, Legre-Boyer V, et al. Correction to: Intra-articular injections of platelet-rich plasma in symptomatic knee osteoarthritis: a consensus statement from French-speaking experts. Knee Surg Sports Traumatol Arthrosc. 2021;29(10):3211-3222. doi: 10.1007/s00167-020-06331-8.
18. Ihnatouski M, Pauk J, Karev B, Karev D. Nanomechanical Properties of Articular Cartilage Due to the PRP Injection in Experimental Osteoarthritis in Rabbits. Molecules. 2020;25(16). doi: 10.3390/molecules25163734.
19. Riboh JC, Saltzman BM, Yanke AB, Fortier L, Cole BJ. Effect of Leukocyte Concentration on the Efficacy of Platelet-Rich Plasma in the Treatment of Knee Osteoarthritis. Am J Sports Med. 2016;44(3):792-800. doi: 10.1177/0363546515580787.
20. Vinod E, Amirtham SM, Kachroo U, Goyal A, Ozbey O, James JV, et al. Articular chondroprogenitors in platelet rich plasma for treatment of osteoarthritis and osteochondral defects in a rabbit knee model. Knee. 2021;30:51-62. doi: 10.1016/j.knee.2021.03.010.
21. Landesberg R, Roy M, Glickman RS. Quantification of growth factor levels using a simplified method of platelet-rich plasma gel preparation. J Oral Maxillofac Surg. 2000;58(3):297-300; discussion -1. doi: 10.1016/s0278-2391(00)90058-2.
22. Pelletier JP, Jovanovic D, Fernandes JC, Manning P, Connor JR, Currie MG, et al. Reduced progression of experimental

osteoarthritis in vivo by selective inhibition of inducible nitric oxide synthase. Arthritis Rheum. 1998;41(7):1275-1286. doi: 10.1002/1529-0131(199807)41:7<1275::AID-ART19>3.0.CO;2-T.
23. Mankin HJ, Johnson ME, Lippiello L. Biochemical and metabolic abnormalities in articular cartilage from osteoarthritic human hips. III. Distribution and metabolism of amino sugar-containing macromolecules. J Bone Joint Surg Am. 1981;63(1):131-9.
24. Wang T, He C. Pro-inflammatory cytokines: The link between obesity and osteoarthritis. Cytokine Growth Factor Rev. 2018;44:38-50. doi: 10.1016/j.cytogfr.2018.10.002.
25. Loeser RF, Collins JA, Diekman BO. Ageing and the pathogenesis of osteoarthritis. Nat Rev Rheumatol. 2016;12(7):412-420. doi: 10.1038/nrrheum.2016.65.
26. Holers VM, Frank RM, Clauw A, Seifert J, Zuscik M, Asokan S, et al. Potential causal role of synovial complement system activation in the development of post-traumatic osteoarthritis after anterior cruciate ligament injury or meniscus tear. Front Immunol. 2023;14:1146563. doi: 10.3389/fimmu.2023.1146563.
27. Jia L, Chen J, Wang Y, Liu Y, Zhang Y, Chen W. Magnetic resonance imaging of osteophytic, chondral, and subchondral structures in a surgically-induced osteoarthritis rabbit model. PLoS One. 2014;9(12):e113707. doi: 10.1371/journal.pone.0113707.
28. Huang L, Riihioja I, Tanska P, Ojanen S, Palosaari S, Kroger H, et al. Early changes in osteochondral tissues in a rabbit model of post-traumatic osteoarthritis. J Orthop Res. 2021;39(12):2556-2567. doi: 10.1002/jor.25009.
29. Havdrup T, Telhag H. Papain-induced changes in the knee joints of adult rabbits. Acta Orthop Scand. 1977;48(2):143-149. doi: 10.3109/17453677708985125.
30. Hermeto LC, Rossi R, Jardim PH, Santana AE, Rinaldi JC, Justulin LA. Comparison between two different experimental models of osteoarthritis in rabbits. Intra-articular collagenase injection and anterior cruciate ligament transection. Acta Cir Bras. 2016;31(9):602-607. doi: 10.1590/S0102-865020160090000005.
31. Everts P, Onishi K, Jayaram P, Lana JF, Mautner K. Platelet-Rich Plasma: New Performance Understandings and Therapeutic Considerations in 2020. Int J Mol Sci. 2020;21(20). doi: 10.3390/ijms21207794.
32. Riewruja K, Phakham S, Sompolpong P, Reantragoon R, Tanavalee A, Ngarmukos S, et al. Cytokine Profiling and Intra-Articular Injection of Autologous Platelet-Rich Plasma in Knee Osteoarthritis. Int J Mol Sci. 2022;23(2). doi: 10.3390/ijms23020890.
33. Moussa M, Lajeunesse D, Hilal G, El Atat O, Haykal G, Serhal R, et al. Platelet rich plasma (PRP) induces chondroprotection via increasing autophagy, anti-inflammatory markers, and decreasing apoptosis in human osteoarthritic cartilage. Exp Cell Res. 2017;352(1):146-156. doi: 10.1016/j.yexcr.2017.02.012.
34. Ragni E, Perucca Orfei C, De Luca P, Libonati F, de Girolamo L. Tissue-Protective and Anti-Inflammatory Landmark of PRP-Treated Mesenchymal Stromal Cells Secretome for Osteoarthritis. Int J Mol Sci. 2022;23(24). doi: 10.3390/ijms232415908.
35. Beigi MH, Atefi A, Ghanaei HR, Labbaf S, Ejeian F, Nasr-Esfahani MH. Activated platelet-rich plasma improves cartilage regeneration using adipose stem cells encapsulated in a 3D alginate scaffold. J Tissue Eng Regen Med. 2018;12(6):1327-1338. doi: 10.1002/term.2663.
36. Liu J, Song W, Yuan T, Xu Z, Jia W, Zhang C. A comparison between platelet-rich plasma (PRP) and hyaluronate acid on the healing of cartilage defects. PLoS One. 2014;9(5):e97293. doi: 10.1371/journal.pone.0097293.
37. Peng YN, Chen JL, Hsu CC, Chen CPC, Suputtitada A. Intra-Articular Leukocyte-Rich Platelet-Rich Plasma versus Intra-Articular Hyaluronic Acid in the Treatment of Knee Osteoarthritis: A Meta-Analysis of 14 Randomized Controlled Trials. Pharmaceuticals (Basel). 2022;15(8). doi: 10.3390/ph15080974.
38. Wang Z, Wang R, Xiang S, Gu Y, Xu T, Jin H, et al. Assessment of the effectiveness and satisfaction of platelet-rich plasma compared with hyaluronic acid in knee osteoarthritis at minimum 7-year follow-up: A post hoc analysis of a randomized controlled trial. Front Bioeng Biotechnol. 2022;10:1062371. doi: 10.3389/fbioe.2022.1062371.
39. Dohan Ehrenfest DM, Rasmusson L, Albrektsson T. Classification of platelet concentrates: from pure platelet-rich plasma (P-PRP) to leucocyte- and platelet-rich fibrin (L-PRF). Trends Biotechnol. 2009;27(3):158-167. doi: doi: 10.1016/j.tibtech.2008.11.009.
40. Tamimi FM, Montalvo S, Tresguerres I, Blanco Jerez L. A comparative study of 2 methods for obtaining platelet-rich plasma. J Oral Maxillofac Surg. 2007;65(6):1084-1093. doi: doi: 10.1016/j.joms.2006.09.012.
41. Nagata MJ, Messora MR, Furlaneto FA, Fucini SE, Bosco AF, Garcia VG, et al. Effectiveness of two methods for preparation of autologous platelet-rich plasma: an experimental study in rabbits. Eur J Dent. 2010;4(4):395-402.
42. Piao L, Park H, Jo CH. Theoretical prediction and validation of cell recovery rates in preparing platelet-rich plasma through a centrifugation. PLoS One. 2017;12(11):e0187509. doi: 10.1371/journal.pone.0187509.
43. Ozer K, Kankaya Y, Colak O, Kocer U. The Impact of Duration and Force of Centrifugation on Platelet Content and Mass in the Preparation of Platelet-Rich Plasma. Aesthetic Plast Surg. 2019;43(4):1078-84. doi: 10.1007/s00266-019-01375-9.
44. Charousset C, Zaoui A, Bellaiche L, Bouyer B. Are multiple platelet-rich plasma injections useful for treatment of chronic patellar tendinopathy in athletes? a prospective study. Am J Sports Med. 2014;42(4):906-911. doi: 10.1177/0363546513519964.
45. Harrison TE, Bowler J, Levins TN, Cheng AL, Reeves KD. Platelet yield and yield consistency for six single-spin methods of platelet rich plasma preparation. Platelets. 2020;31(5):661-666. doi: 10.1080/09537104.2019.1663808.
46. Jayaram P, Liu C, Dawson B, Ketkar S, Patel SJ, Lee BH, et al. Leukocyte-dependent effects of platelet-rich plasma on cartilage loss and thermal hyperalgesia in a mouse model of post-traumatic osteoarthritis. Osteoarthritis Cartilage. 2020;28(10):1385-1393. doi: 10.1016/j.joca.2020.06.004.
47. Di Martino A, Boffa A, Andriolo L, Romandini I, Altamura SA, Cenacchi A, et al. Leukocyte-Rich versus Leukocyte-Poor Platelet-Rich Plasma for the Treatment of Knee Osteoarthritis: A Double-Blind Randomized Trial. Am J Sports Med. 2022;50(3):609-617. doi: 10.1177/03635465211064303.
48. Lana JF, Macedo A, Ingrao ILG, Huber SC, Santos GS, Santana MHA. Leukocyte-rich PRP for knee osteoarthritis: Current concepts. J Clin Orthop Trauma. 2019;10(Suppl 1):S179-S182. doi: 10.1016/j.jcot.2019.01.011.
49. Tschaikowsky M, Brander S, Barth V, Thomann R, Rolauffs B, Balzer BN, et al. The articular cartilage surface is impaired by a loss of thick collagen fibers and formation of type I collagen in early osteoarthritis. Acta Biomater. 2022;146:274-283. doi: doi: 10.1016/j.actbio.2022.04.036.
50. Sadigursky D, Magnavita VFS, Sa CKC, Monteiro HS, Braghiroli OFM, Matos MAA. Undenatured Collagen Type Ii for the Treatment of Osteoarthritis of the Knee. Acta Ortop Bras. 2022;30(2):e240572. doi: 10.1590/1413-785220223002240572.
51. Xu R, Wu J, Zheng L, Zhao M. Undenatured type II collagen and its role in improving osteoarthritis. Ageing Res Rev. 2023;91:102080. doi: 10.1016/j.arr.2023.102080.
52. Orhan C, Juturu V, Sahin E, Tuzcu M, Ozercan IH, Durmus AS, et al. Undenatured Type II Collagen Ameliorates Inflammatory

Responses and Articular Cartilage Damage in the Rat Model of Osteoarthritis. Front Vet Sci. 2021;8:617789. doi: 10.3389/fvets.2021.617789.

53. Nagata K, Hojo H, Chang SH, Okada H, Yano F, Chijimatsu R, et al. Runx2 and Runx3 differentially regulate articular chondrocytes during surgically induced osteoarthritis development. Nat Commun. 2022;13(1):6187. doi: 10.1038/s41467-022-33744-5.
54. Ding DF, Xue Y, Zhang JP, Zhang ZQ, Li WY, Cao YL, et al. Similarities and differences between rat and mouse chondrocyte gene expression induced by IL-1beta. J Orthop Surg Res. 2022;17(1):70. doi: 10.1186/s13018-021-02889-2.
55. Niemiec P, Szyluk K, Balcerzyk A, Kalita M, Jarosz A, Iwanicka J, et al. Why PRP works only on certain patients with tennis elbow? Is PDGFB gene a key for PRP therapy effectiveness? A prospective cohort study. BMC Musculoskelet Disord. 2021;22(1):710. doi: 10.1186/s12891-021-04593-y.